World Journal of Advanced Engineering Technology and Sciences
eISSN: 2582-8266
Cross Ref DOI: 10.30574/wjaets
Journal homepage: https://wjaets.com/

(RESEARCH ARTICLE)

Check for updates

Synthesis, characterization and adsorption performance of biomass-derived adsorbents for heavy metal removal from water

Oyibocha Alick David *

Department of Chemical Engineering, Lagos State University of Science and Technology, (Formerly Lagos State Polytechnic) Nigeria.

World Journal of Advanced Engineering Technology and Sciences, 2026, 19(01), 022-034

Publication history: Received on 24 February 2026; revised on 31 March 2026; accepted on 02 April 2026

Article DOI: https://doi.org/10.30574/wjaets.2026.19.1.0188

Abstract

Heavy-metal pollution in water remains a major environmental and health concern because these contaminants are toxic, persistent, and able to accumulate in living organisms. This study examined the preparation, characterization, and adsorption behavior of adsorbents produced from agricultural biomass for the removal of toxic metals from aqueous media. The biomass precursor was converted into activated carbon through phosphoric-acid activation. The resulting material was characterized by FTIR, SEM, and BET surface-area analysis to determine its surface chemistry, morphology, and pore properties. Batch adsorption tests were then performed to assess the removal of Pb(II), Cd(II), and Cr(VI) under different operating conditions, including pH, contact time, initial concentration, adsorbent dosage, and temperature. The adsorbent exhibited strong removal performance, with equilibrium data best represented by the Langmuir model and kinetic behavior aligning more closely with the pseudo-second-order model. Thermodynamic evaluation also indicated that adsorption occurred spontaneously. Overall, the findings suggest that biomass-derived activated carbon offers a low-cost and sustainable option for treating metal-contaminated water.

Keywords: Biomass-derived adsorbent; Heavy metals; Activated carbon; Adsorption isotherm; Water treatment; Chemical activation

1. Introduction

Water Heavy metal pollution in water continues to be one of the most pressing environmental issues because of its harmful effects on human health, aquatic life, and long-term water sustainability [1], [4]. Metals such as lead (Pb), cadmium (Cd), and chromium (Cr) are particularly dangerous since they remain in the environment for long periods, resist biodegradation, and can accumulate progressively in living systems [1], [4]. Their occurrence in water bodies is often linked to industrial operations such as mining, electroplating, tanning, battery production, pigment manufacturing, and metal finishing [1], [12]. Once released into aquatic environments, these contaminants may enter the food chain and contribute to serious health problems including neurological damage, kidney malfunction, skeletal abnormalities, and carcinogenic effects [4], [18]. Conventional methods for removing heavy metals from wastewater include chemical precipitation, ion exchange, coagulation-flocculation, membrane filtration, and electrochemical treatment [1], [5], [12]. Although these approaches can be effective under certain conditions, they are often associated with disadvantages such as high operating costs, reduced efficiency at low metal concentrations, membrane fouling, and the generation of sludge that requires additional treatment and disposal [1], [12], [16]. These limitations have increased interest in treatment options that are both more economical and more environmentally sustainable. Among the available treatment technologies, adsorption has become one of the most attractive approaches for heavy metal removal because it is simple to operate, adaptable, efficient, and well suited for dilute solutions [1], [2], [7]. Activated carbon is widely recognized as a highly effective adsorbent due to its large surface area, porous structure, and abundance of

* Corresponding author: Oyibocha Alick David.

reactive surface functional groups [9], [10]. However, the widespread use of commercial activated carbon is constrained by the relatively high cost of production and regeneration [1], [16]. For this reason, attention has increasingly shifted toward low-cost adsorbents prepared from naturally abundant biomass and agricultural wastes. Biomass-based adsorbents have gained significant interest because they are renewable, inexpensive, readily available, and environmentally friendly [4], [9], [10]. Agricultural by-products such as rice husk, coconut shell, sawdust, apricot stone, tamarind wood, and hazelnut husk have all been explored as precursors for activated carbon and related adsorbent materials [9], [13]-[16]. These raw materials contain lignocellulosic constituents, mainly cellulose, hemicellulose, and lignin, which provide a suitable carbon framework for producing porous adsorbents after controlled thermal and chemical treatment [4], [10]. Their utilization not only lowers adsorbent production costs but also promotes waste valorization and sustainable resource use [10], [16]. Rice husk is particularly promising as a precursor for adsorbent synthesis because it is produced in large quantities as a by-product of rice processing and is often discarded through open burning or landfilling [4]. Its abundance, low market value, carbon-rich composition, and silica content make it an appropriate raw material for activated carbon production [4], [9]. Previous studies have shown that activated carbons derived from agricultural biomass can display strong adsorption capacities for a range of pollutants, including heavy metals, depending on the activation route, carbonization conditions, and surface chemistry of the final product [9], [13]-[15].

The adsorption efficiency of biomass-derived activated carbon is strongly affected by the activation method used during preparation. Chemical activation is widely regarded as an effective strategy for generating adsorbents with enhanced porosity and improved surface functionality [9]-[11]. Among various activating agents, phosphoric acid has been extensively applied because it promotes dehydration, bond cleavage, cross-linking, and pore development within lignocellulosic materials during carbonization [11]. In addition, phosphoric acid treatment can introduce oxygen-containing functional groups such as hydroxyl, carbonyl, and carboxyl groups onto the adsorbent surface, which play important roles in heavy metal binding through electrostatic attraction, ion exchange, and surface complexation [4], [11]. The adsorption of heavy metals onto solid surfaces is commonly interpreted using equilibrium, kinetic, and thermodynamic models. The Langmuir and Freundlich isotherm models are frequently used to explain adsorption equilibrium behavior [2], [7]. Likewise, pseudo-first-order and pseudo-second-order kinetic models are commonly employed to evaluate adsorption rates and possible controlling mechanisms, with the pseudo-second-order model often providing a stronger fit in heavy metal adsorption systems [3]. Thermodynamic parameters such as Gibbs free energy, enthalpy, and entropy are also useful for assessing whether adsorption is spontaneous and energetically favorable [7], [8]. Together, these models provide an important basis for evaluating the performance of newly developed biomass-derived adsorbents. Despite the large amount of published work on low-cost adsorbents, further study is still needed on locally available agricultural wastes and their conversion into effective materials for water treatment. In this study, rice husk was selected as the precursor for producing biomass-derived activated carbon through phosphoric acid activation. The resulting material was characterized and then tested for the removal of Pb(II), Cd(II), and Cr(VI) from aqueous solution. The effects of pH, contact time, initial concentration, adsorbent dosage, and temperature were investigated, while isotherm, kinetic, and thermodynamic analyses were used to explain the adsorption process. The study therefore aimed to demonstrate the potential of rice-husk-derived activated carbon as a sustainable, low-cost, and efficient adsorbent for heavy metal remediation in water treatment systems.

2. Materials and Methods

2.1. Materials and Reagents

Rice husk (RH) was selected as the raw biomass for producing activated carbon. The raw material was washed thoroughly with tap water and then rinsed several times with deionized (DI) water to remove dust and surface impurities. After cleaning, the sample was dried in an oven at 105 °C for 24 h, milled, and sieved to obtain particles of ≤500 μm. Phosphoric acid (H_3PO_4, 85 wt%) was used as the activating chemical. Lead nitrate [$Pb(NO_3)_2$], cadmium chloride dihydrate ($CdCl_2 \cdot 2H_2O$), and potassium dichromate ($K_2Cr_2O_7$) served as the precursor compounds for Pb(II), Cd(II), and Cr(VI), respectively. All reagents were of analytical grade and were used without additional purification. All aqueous solutions were prepared using deionized water with a resistivity of at least 18 MΩ·cm.

2.2. Preparation of Biomass-Derived Activated Carbon

Biomass-derived activated carbon (BAC) was produced from rice husk through a sequence of pre-treatment, pre-carbonization, chemical activation, carbonization, washing, and final particle-size reduction. A schematic summary of the preparation route is presented in Figure 1.

2.2.1. Pre-treatment and Pre-carbonization

The cleaned and dried rice husk was first pre-carbonized in a muffle furnace at 300 °C for 60 min under oxygen-restricted conditions in a covered ceramic crucible. The heating rate during this stage was maintained at 10 °C min^{-1}.

2.2.2. Chemical Activation and Carbonization

The pre-carbonized material was impregnated with phosphoric acid at a mass ratio of 1:1 (H_3PO_4:char, w/w). The mixture was stirred continuously for 4 h and then left for 12 h to allow proper penetration of the activating agent into the carbon structure. The impregnated sample was then dried at 110 °C for 12 h. After drying, carbonization was carried out in a muffle furnace at 600 °C for 2 h under oxygen-limited conditions, using a heating rate of 10 °C min^{-1}. The carbonized product was washed repeatedly with hot deionized water until the washings reached approximately neutral pH (pH ≈ 7), ensuring removal of residual phosphoric acid and other soluble impurities. The washed material was dried again at 105 °C for 24 h, ground, and sieved to obtain particles within the range of 100–250 µm. The final adsorbent was designated as biomass-derived activated carbon (BAC) and stored in a desiccator until use.

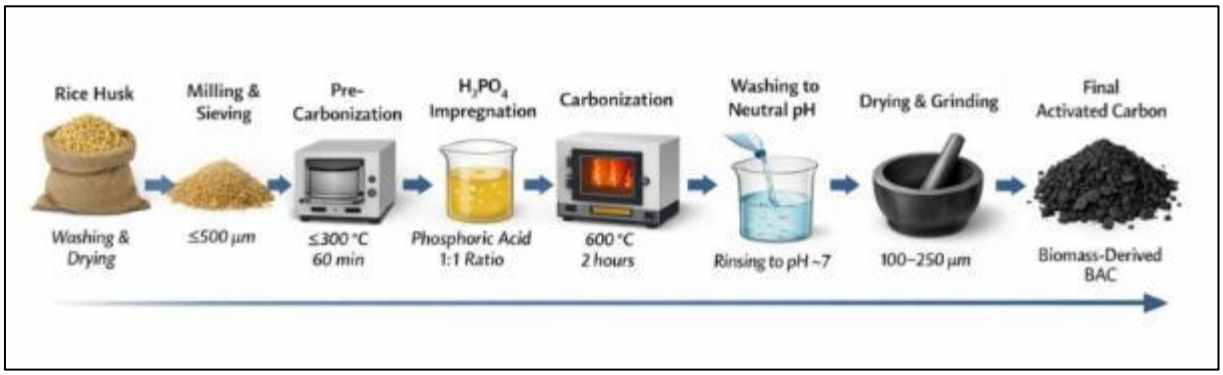

Figure 1 Schematic representation of the preparation of biomass-derived activated carbon (BAC) from rice husk through washing, drying, milling, pre-carbonization, phosphoric acid impregnation, carbonization, washing to neutral pH, and final grinding

2.3. Characterization of the Adsorbent

The functional groups present on the BAC surface were analyzed using Fourier Transform Infrared Spectroscopy (FTIR) over the wavenumber range of 4000–400 cm^{-1}. Surface morphology and pore development were examined by Scanning Electron Microscopy (SEM) after coating the samples with gold. The specific surface area, pore volume, and average pore diameter were determined using Brunauer-Emmett-Teller (BET) analysis based on nitrogen adsorption-desorption isotherms at 77 K, after degassing the samples at 200 °C for 4 h. The pH at the point of zero charge (pH_pzc) was measured using the pH drift method. In this procedure, 0.01 M NaCl solution was prepared and adjusted to initial pH values ranging from 2 to 12 using 0.1 M HCl or 0.1 M NaOH. Approximately 0.1 g of BAC was added to 50 mL of each solution and left to equilibrate for 24 h. The final pH values were then recorded, and the pH_pzc was determined from the relationship between the initial and final pH values.

2.4. Preparation of Metal Ion Solutions

Stock solutions of Pb(II), Cd(II), and Cr(VI), each at a concentration of 1000 mg L^{-1}, were prepared by dissolving accurately weighed amounts of $Pb(NO_3)_2$, $CdCl_2 \cdot 2H_2O$, and $K_2Cr_2O_7$, respectively, in deionized water. Working solutions with concentrations between 10 and 200 mg L^{-1} were obtained by serial dilution of the stock solutions. Before each adsorption experiment, the pH of the working solution was adjusted to the required value using 0.1 M HCl or 0.1 M NaOH.

2.5. Batch Adsorption Experiments

Batch adsorption studies were conducted in 250 mL Erlenmeyer flasks containing 100 mL of metal ion solution and a measured quantity of adsorbent. The flasks were shaken in a thermostatic orbital shaker at 150 rpm. All experiments were performed in triplicate, and the reported values represent the averages obtained. The effects of contact time (0–180 min), initial metal ion concentration (10–200 mg L^{-1}), solution pH (2–8), adsorbent dosage (0.25–1.50 g L^{-1}), and temperature (25–45 °C) were systematically evaluated. After adsorption, the suspensions were filtered using Whatman filter paper, and the resulting filtrates were analyzed for residual metal ion concentration.

2.6. Analytical Determination

The remaining concentrations of Pb(II), Cd(II), and Cr(VI) in the filtrates were measured using Atomic Absorption Spectroscopy (AAS). Calibration curves were prepared with standard solutions, and only calibration plots with correlation coefficients of $R^2 \geq 0.999$ were accepted for quantitative analysis.

The equilibrium adsorption capacity, q_e(mg g^{-1}), and percentage removal, %R, were calculated using Eqs. (1) and (2), respectively:

$$q_e = \frac{(C_0 - C_e)V}{m} \qquad (1)$$

$$\%R = \frac{(C_0 - C_e)}{C_0} \times 100 \qquad (2)$$

where C_0 and C_e denote the initial and equilibrium concentrations of the metal ion (mg L^{-1}), respectively, V is the solution volume (L), and m is the mass of adsorbent (g).

For kinetic analysis, the adsorption capacity at time t, q_t, was calculated using Eq. (3):

$$q_t = \frac{(C_0 - C_t)V}{m} \qquad (3)$$

where C_t is the concentration of the metal ion at time t (mg L^{-1}).

2.7. Adsorption Isotherm and Kinetic Modeling

The equilibrium adsorption results were interpreted using the Langmuir and Freundlich isotherm models. The adsorption kinetics were analyzed using pseudo-first-order (PFO) and pseudo-second-order (PSO) models. Model parameters were obtained through linear regression, and the quality of fit was evaluated using the correlation coefficient (R^2).

2.8. Thermodynamic Analysis

Thermodynamic parameters were determined from adsorption data collected at different temperatures. The Gibbs free energy change, ΔG°, was calculated using Eq. (4):

$$\Delta G^\circ = -RT \ln K_c \qquad (4)$$

where R is the universal gas constant (8.314 J mol^{-1} K^{-1}), T is the absolute temperature (K), and K_c is the equilibrium constant. The enthalpy change, ΔH°, and entropy change, ΔS°, were obtained from the Van't Hoff equation by plotting $\ln K_c$ against $1/T$.

3. Results

3.1. Characterization of the Adsorbent

The physicochemical characteristics of the biomass-derived activated carbon (BAC) prepared from rice husk are presented in Table 1. The BET surface area of the adsorbent was 512 m^2 g^{-1}, while the pore volume and average pore diameter were 0.41 cm^3 g^{-1} and 3.2 nm, respectively. These values indicate that phosphoric acid activation was effective in producing a porous adsorbent structure with a sufficiently high surface area for heavy metal uptake. Since adsorption is a surface-dependent process, the relatively high BET surface area suggests that BAC possesses a large number of accessible active sites for interaction with dissolved metal ions.

The average pore diameter of 3.2 nm indicates that the adsorbent is predominantly mesoporous. This pore structure is beneficial because mesopores facilitate the transport of hydrated metal ions from the bulk solution into the interior adsorption regions, while the overall pore volume supports adequate diffusion and retention of adsorbates. The combination of high surface area and suitable pore size therefore confirms that the synthesized adsorbent has favorable textural properties for aqueous-phase adsorption.

The pH at the point of zero charge (pH_pzc) of BAC was found to be 6.1. This parameter is important because it reflects the pH at which the surface carries zero net charge. At pH values below 6.1, the BAC surface is expected to be positively

charged, whereas at pH values above 6.1, the surface becomes negatively charged. Consequently, adsorption of cationic species such as Pb(II) and Cd(II) is expected to be more favorable near or above this pH due to reduced electrostatic repulsion and enhanced attraction toward negatively charged surface sites.

Table 1 Expanded physicochemical properties of biomass-derived activated carbon (BAC)

Parameter	Value	Observation	Interpretation	Implication for adsorption
BET surface area ($m^2\ g^{-1}$)	512	Relatively high surface area	Phosphoric acid activation effectively generated porous carbon	Provides abundant active sites for heavy metal uptake
Pore volume ($cm^3\ g^{-1}$)	0.41	Appreciable internal pore space	Indicates well-developed void structure	Enhances diffusion of ions into the adsorbent matrix
Average pore diameter (nm)	3.2	Mesoporous structure	Suitable for transport of hydrated metal ions	Improves accessibility of adsorption sites
pH at point of zero charge (pH_pzc)	6.1	Surface charge changes near pH 6	Surface becomes negatively charged above this value	Favors adsorption of cationic metals at near-neutral pH

The FTIR spectral assignments shown in Table 2 confirm the presence of several oxygen-containing functional groups on the BAC surface, including hydroxyl, carbonyl, and C–O groups. These groups are particularly important in adsorption because they can participate in metal binding through electrostatic attraction, coordination, ion exchange, and surface complexation. The aromatic C=C band further indicates the formation of carbonaceous structures during carbonization, while the aliphatic C–H band suggests retention of some organic structural features.

Table 2 Expanded FTIR functional groups identified on BAC surface

Wavenumber (cm^{-1})	Functional group	Assignment	Role in adsorption	Likely interaction with metal ions
~3420	–OH	Hydroxyl stretching	Provides polar active sites	Hydrogen bonding, complexation, electrostatic attraction
~2920	C–H	Aliphatic stretching	Indicates residual carbon backbone structure	Minor direct contribution to adsorption
~1720	C=O	Carbonyl	Reactive oxygen-containing group	Surface complexation and coordination with metal ions
~1620	C=C	Aromatic	Carbonized aromatic structure	Contributes to adsorbent framework stability
~1100	C–O	Alcohol/ether	Oxygenated surface functionality	Ion exchange and coordination with dissolved metals

The presence of these oxygenated groups suggests that the adsorption mechanism is not governed by pore filling alone, but also involves chemical interaction between heavy metal ions and the adsorbent surface. This is further supported by the proposed adsorption mechanism shown in Figure 2.

SEM observations revealed that the chemical activation and carbonization processes created a rough, irregular, and porous surface. The visible cavities and channels formed on the BAC surface indicate that volatile substances were removed during thermal treatment, leaving behind a developed pore system. Such morphology enhances the diffusion of metal ions into the adsorbent and increases the likelihood of contact between adsorbates and active binding sites. Overall, the characterization results confirm that the rice husk-derived BAC possesses suitable textural and chemical properties for effective adsorption of heavy metals from water.

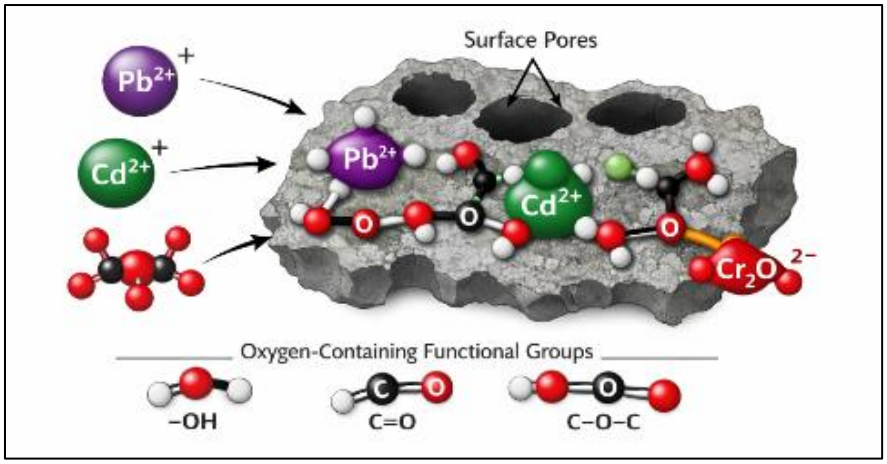

Figure 2 Proposed adsorption mechanism of Pb(II), Cd(II), and Cr(VI) onto biomass-derived activated carbon. showing the role of surface pores and oxygen-containing functional groups such as hydroxyl, carbonyl, and ether groups

3.2. Effect of Contact Time on Pb(II) Adsorption

The effect of contact time on Pb(II) adsorption onto BAC is presented in Table 3 and Figure 2. The data show that adsorption occurred rapidly during the early stage of the process and then gradually approached equilibrium. At 10 min, the removal efficiency had already reached 38.5%, corresponding to an adsorption capacity of 3.85 mg g^{-1}. This rapid initial uptake can be attributed to the large number of vacant active sites available on the external surface of the adsorbent at the beginning of the experiment.

As contact time increased, the removal efficiency rose steadily to 82.4% at 60 min and then approached 89.3% at 180 min. Similarly, the adsorption capacity increased from 0.00 mg g^{-1} at 0 min to 8.93 mg g^{-1} at 180 min. The increase was much more pronounced during the first 60 min than during the later period, indicating that the adsorption process occurred in two distinct stages.

Table 3 Expanded effect of contact time on Pb(II) adsorption onto BAC

Time (min)	Ce (mg L^{-1})	Removal (%)	q_t (mg g^{-1})	Increment in removal (%)	Adsorption stage	Interpretation
0	100.0	0.0	0.00	–	Initial	No adsorption has occurred
10	61.5	38.5	3.85	38.5	Rapid uptake	Many vacant active sites available
20	44.2	55.8	5.58	17.3	Rapid uptake	Strong concentration gradient drives adsorption
30	31.8	68.2	6.82	12.4	Rapid uptake	Continued occupation of available sites
45	22.4	77.6	7.76	9.4	Intermediate	Surface sites begin to fill
60	17.6	82.4	8.24	4.8	Intermediate	Adsorption rate slows as sites are consumed
90	13.5	86.5	8.65	4.1	Slower phase	Intraparticle diffusion becomes important
120	11.8	88.2	8.82	1.7	Near equilibrium	Adsorption approaches steady state
150	11.0	89.0	8.90	0.8	Equilibrium region	Minimal additional uptake occurs
180	10.7	89.3	8.93	0.3	Equilibrium	System has essentially reached equilibrium

During the first stage, adsorption was dominated by surface interaction and external mass transfer, aided by the high concentration gradient between the Pb(II) solution and the BAC surface. During the second stage, the rate of adsorption slowed because the most accessible sites were already occupied and the remaining ions had to diffuse into less accessible internal pores. This later stage is commonly associated with intraparticle diffusion and site saturation.

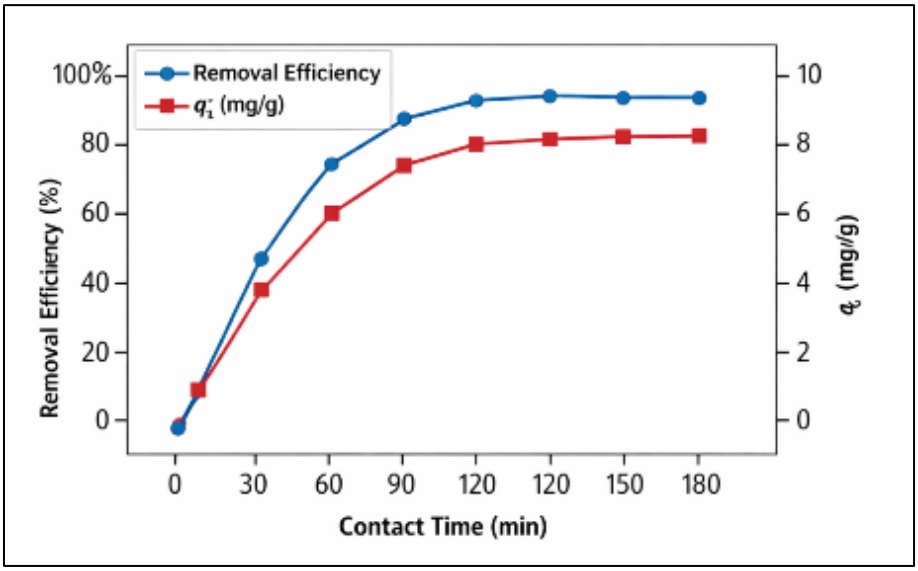

Figure 3 Effect of contact time on Pb(II) adsorption onto biomass-derived activated carbon

The slight increase in removal efficiency after 120 min indicates that equilibrium was nearly attained within this period. Therefore, 120 min may be considered an appropriate equilibrium contact time for subsequent adsorption studies. The overall behavior supports the later kinetic analysis, which showed that the pseudo-second-order model best described the adsorption process.

3.3. Effect of pH on Pb(II) Adsorption

The effect of solution pH on Pb(II) adsorption is shown in Table 4 and Figure 3. The results demonstrate that pH had a strong influence on the adsorption performance of BAC. At pH 2, the removal efficiency was only 27.5%, with an adsorption capacity of 2.75 mg g^{-1}. Under such strongly acidic conditions, the high concentration of H^+ ions competes with Pb(II) ions for the active sites on the adsorbent surface, thereby suppressing adsorption.

Table 4 Expanded effect of pH on Pb(II) adsorption onto BAC

pH	Removal (%)	q_e (mg g^{-1})	Surface condition	Dominant effect	Interpretation
2	27.5	2.75	Highly protonated surface	Strong H^+ competition	Poor adsorption due to limited available negative sites
3	48.2	4.82	Protonated surface	Reduced proton competition	Adsorption begins to improve
4	70.4	7.04	Less protonated surface	Increasing attraction for Pb(II)	More active sites become available
5	85.2	8.52	Near favorable range	Strong electrostatic interaction	Major increase in Pb(II) uptake
6	88.5	8.85	Around pH_pzc	Optimum adsorption condition	Best balance between surface charge and metal stability
7	87.4	8.74	Slightly negative surface	High adsorption maintained	Slight decrease possibly due to Pb species changes
8	83.1	8.31	More negative surface	Possible hydroxide formation	Apparent adsorption decreases slightly

As the pH increased from 2 to 6, the adsorption performance improved markedly. Removal efficiency rose from 27.5% to 88.5%, while adsorption capacity increased from 2.75 to 8.85 mg g^{-1}. This trend can be explained by reduced proton competition and the gradual deprotonation of surface functional groups, which creates more negatively charged sites capable of attracting Pb(II) ions.

The highest removal was observed at pH 6, which is very close to the measured pH_pzc of 6.1. This suggests that surface charge behavior played a major role in the adsorption process. At this pH, the BAC surface becomes favorable for the adsorption of cationic Pb(II), while the metal remains sufficiently stable in solution for adsorption to occur efficiently.

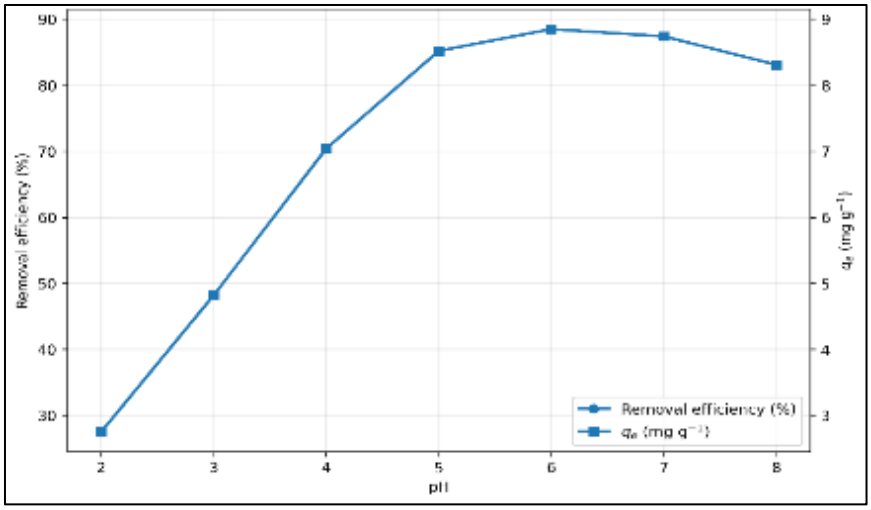

Figure 4 Effect of solution pH on Pb(II) adsorption onto biomass-derived activated carbon

At pH 7 and 8, a slight decrease in removal efficiency was observed. This decline may be associated with changes in lead speciation and the possible onset of lead hydroxide formation at higher pH values. Although adsorption remained high, pH 6 was identified as the optimum pH for Pb(II) removal in this study.

3.4. Effect of Initial Concentration on Pb(II) Adsorption

Table 5 Expanded effect of initial Pb(II) concentration on adsorption onto BAC

C_0 (mg L^{-1})	Removal (%)	q_e (mg g^{-1})	Trend in removal	Trend in capacity	Interpretation
10	91.0	0.91	Highest removal	Lowest capacity	Few ions relative to available sites
25	86.4	2.16	Slightly lower	Increased capacity	More ions available for uptake
50	83.8	4.19	Decreasing	Increasing	Higher concentration gradient improves loading
75	80.1	6.01	Decreasing	Increasing	Greater site occupation per unit mass
100	88.2	8.82	Slight irregular rise	Increasing	Possible experimental variation
150	76.9	11.53	Lower	High capacity	Site saturation becomes more evident
200	70.3	14.06	Lowest removal	Highest capacity	Maximum loading reached, but fewer ions removed proportionally

The influence of initial Pb(II) concentration on adsorption performance is summarized in Table 5. As the initial concentration increased from 10 to 200 mg L^{-1}, the adsorption capacity increased from 0.91 to 14.06 mg g^{-1}. This trend shows that a higher initial metal concentration provides a stronger driving force for mass transfer, allowing more Pb(II) ions to be adsorbed per unit mass of BAC.

At the same time, the percentage removal generally decreased with increasing concentration, from 91.0% at 10 mg L^{-1} to 70.3% at 200 mg L^{-1}. This is because the number of available adsorption sites on the BAC surface is limited. At low concentrations, the ratio of active sites to dissolved ions is high, allowing a larger fraction of Pb(II) to be removed. At higher concentrations, these sites progressively approach saturation, so a smaller proportion of the total ions can be adsorbed even though the absolute amount adsorbed increases.

The slight irregular increase in removal efficiency at 100 mg L^{-1} may reflect experimental variability. Nevertheless, the overall pattern remains clear: higher initial concentrations favor greater adsorption capacity but lower percentage removal. This indicates that BAC can carry larger Pb(II) loads at high concentration, though with reduced proportional efficiency.

3.5. Effect of Adsorbent Dosage

The effect of adsorbent dosage on Pb(II) removal is presented in Table 6. Increasing the BAC dosage from 0.25 to 1.50 g L^{-1} led to an increase in removal efficiency from 51.4% to 92.2%. This is expected because a higher adsorbent dosage introduces more total surface area and more binding sites into the system. However, the adsorption capacity decreased from 20.56 to 6.15 mg g^{-1} as the dosage increased. This inverse relationship is commonly observed in adsorption studies and may be attributed to underutilization of active sites, site overlap, and particle aggregation at higher adsorbent concentrations. In other words, although more total sites are available, not all are fully occupied when the same amount of Pb(II) is distributed over a larger adsorbent mass.

Table 6 Expanded effect of adsorbent dosage on Pb(II) adsorption

Dose (g L^{-1})	Removal (%)	q_e (mg g^{-1})	Surface site availability	Adsorbent utilization	Interpretation
0.25	51.4	20.56	Low total sites	Highest per-unit utilization	Fewer sites overall, but each gram is highly loaded
0.50	70.7	14.14	Moderate	High	More sites improve removal efficiency
0.75	81.3	10.84	Higher	Moderate	Removal improves, but capacity begins to decline
1.00	88.2	8.82	High	Balanced	Good compromise between removal and capacity
1.25	90.8	7.26	Very high	Lower	More sites remain unsaturated
1.50	92.2	6.15	Maximum	Lowest	Highest removal but least efficient per gram

These findings indicate that low adsorbent dosages favor high adsorption capacity per unit mass, while higher dosages favor maximum overall removal efficiency. In practical terms, a dosage of 1.00 g L^{-1} appears to provide a good operational balance between these two objectives.

3.6. Adsorption Isotherm Analysis

The adsorption isotherm parameters for Pb(II), Cd(II), and Cr(VI) are presented in Table 7. For all three ions, the Langmuir model showed higher correlation coefficients than the Freundlich model. The Langmuir R^2 values were 0.992, 0.987, and 0.981 for Pb(II), Cd(II), and Cr(VI), respectively, while the corresponding Freundlich values were 0.964, 0.955, and 0.947. This indicates that the Langmuir model provided a better description of the adsorption equilibrium data. The better fit of the Langmuir model suggests that adsorption occurred predominantly as monolayer coverage on a relatively homogeneous surface, with each active site accommodating one adsorbate species.

Table 7 Expanded isotherm parameters for heavy metal adsorption onto BAC

Metal ion	q_{max} (mg g^{-1})	R^2 (Langmuir)	R^2 (Freundlich)	Better-fitting model	Interpretation	Relative affinity
Pb(II)	16.45	0.992	0.964	Langmuir	Monolayer adsorption on relatively uniform sites	Highest
Cd(II)	13.88	0.987	0.955	Langmuir	Favorable monolayer adsorption	Moderate
Cr(VI)	11.96	0.981	0.947	Langmuir	Adsorption occurs, but lower than Pb(II) and Cd(II)	Lowest

The maximum monolayer capacities followed the order Pb(II) > Cd(II) > Cr(VI). This indicates that BAC had the strongest affinity for Pb(II), likely because of favorable interaction between lead ions and the oxygen-containing surface groups of the adsorbent. The lower uptake of Cr(VI) may be related to its different speciation and adsorption behavior in aqueous solution.

3.7. Kinetic Analysis

The kinetic model fitting results are presented in Table 8. For all studied metal ions, the pseudo-second-order (PSO) model gave higher R^2 values than the pseudo-first-order (PFO) model. For Pb(II), Cd(II), and Cr(VI), the PSO model yielded R^2 values of 0.996, 0.991, and 0.986, respectively, compared with 0.918, 0.907, and 0.894 for the PFO model.

These results indicate that the PSO model better describes the adsorption kinetics, suggesting that the adsorption process may be controlled largely by chemisorption-related interactions involving electron sharing or exchange between metal ions and the BAC surface.

Table 8 Expanded kinetic parameters for heavy metal adsorption onto BAC

Metal ion	R^2 (PFO)	R^2 (PSO)	Better-fitting model	Suggested mechanism	Interpretation
Pb(II)	0.918	0.996	PSO	Chemisorption-dominated	Strong interaction between Pb(II) and BAC surface groups
Cd(II)	0.907	0.991	PSO	Chemisorption-dominated	Adsorption likely controlled by surface reaction
Cr(VI)	0.894	0.986	PSO	Chemisorption-dominated	Slower but still well described by PSO model

The kinetic behavior is consistent with the FTIR findings, which showed the presence of reactive oxygen-containing groups capable of participating in metal binding. However, the contact time results also suggest that diffusion processes contributed to the overall adsorption mechanism, particularly in the later stage of adsorption.

3.8. Thermodynamic Analysis

The thermodynamic parameters presented in Table 9 show that the Gibbs free energy changes (ΔG°) for Pb(II), Cd(II), and Cr(VI) adsorption were negative under the studied conditions. The values were -5.97, -5.49, and -4.67 kJ mol^{-1}, respectively.

The negative sign of ΔG° confirms that the adsorption process was spontaneous for all three metal ions. Among them, Pb(II) exhibited the most negative value, indicating that its adsorption onto BAC was thermodynamically more favorable than that of Cd(II) and Cr(VI).

Table 9 Expanded thermodynamic parameters for heavy metal adsorption onto BAC

Metal ion	ΔG° (kJ mol^{-1})	Sign of ΔG°	Process nature	Relative spontaneity	Interpretation
Pb(II)	-5.97	Negative	Spontaneous	Highest	Adsorption is thermodynamically most favorable for Pb(II)
Cd(II)	-5.49	Negative	Spontaneous	Moderate	BAC shows good affinity toward Cd(II)
Cr(VI)	-4.67	Negative	Spontaneous	Lowest	Adsorption is feasible but less favorable than for Pb(II) and Cd(II)

The order of spontaneity, Pb(II) > Cd(II) > Cr(VI), agrees with the isotherm results and further supports the conclusion that BAC had the highest affinity for Pb(II). Although only ΔG° values are available here, the thermodynamic results still confirm that the adsorption process is feasible and favorable.

4. Discussion

The expanded results clearly demonstrate that rice husk-derived BAC is an effective adsorbent for the removal of heavy metals from aqueous solutions. The characterization data confirmed that the adsorbent possessed a combination of high surface area, mesoporous structure, suitable pore volume, and chemically active oxygen-containing groups. These properties contributed directly to its adsorption performance.

The adsorption experiments showed that Pb(II) uptake was strongly influenced by contact time, pH, initial concentration, and adsorbent dosage. The contact time study revealed a rapid initial uptake followed by a slower equilibrium stage. The pH study showed that adsorption was highly favored near pH 6, in agreement with the measured pH_pzc. The concentration study demonstrated that higher metal concentrations increased adsorption capacity but reduced percentage removal, while the dosage study showed that greater adsorbent mass improved removal efficiency but lowered the amount adsorbed per unit mass. The isotherm, kinetic, and thermodynamic results consistently indicated that Pb(II) showed the highest affinity toward BAC, followed by Cd(II) and Cr(VI). The Langmuir model best described equilibrium behavior, the pseudo-second-order model best described kinetic behavior, and negative Gibbs free energy values confirmed the spontaneous nature of the adsorption process.

5. Conclusion

This study has shown that rice husk can be converted into an effective biomass-derived activated carbon through phosphoric acid activation and thermal carbonization. The adsorbent produced displayed desirable physicochemical properties, including a high BET surface area, considerable pore volume, a mesoporous structure, and oxygen-containing functional groups such as hydroxyl, carbonyl, and C–O groups. These properties contributed to its good performance in removing heavy metals from aqueous solutions. The adsorption experiments also showed that the performance of the material depended strongly on operating conditions such as contact time, pH, initial metal concentration, and adsorbent dosage. Pb(II) removal was rapid at the beginning of the process and reached equilibrium after about 120 min. The best adsorption performance for Pb(II) was obtained at pH 6, where competition from protons was lower and the surface conditions were more suitable for metal uptake. An increase in initial concentration led to higher adsorption capacity, while a higher adsorbent dosage improved removal efficiency but reduced the amount adsorbed per unit mass.

The equilibrium results for Pb(II), Cd(II), and Cr(VI) were better fitted by the Langmuir isotherm model, suggesting mainly monolayer adsorption on a fairly uniform surface. The pseudo-second-order model gave the best fit for the kinetic data, indicating that chemisorption played an important role in the adsorption process. In addition, the negative Gibbs free energy values obtained for all the investigated metals confirmed that adsorption occurred spontaneously under the conditions studied. Among the three metal ions examined, Pb(II) showed the highest affinity for the adsorbent, followed by Cd(II) and Cr(VI). This suggests that the prepared biomass-derived activated carbon is particularly promising for the treatment of lead-contaminated water, while also being useful for the removal of other toxic heavy metals. Overall, rice-husk-derived activated carbon can be regarded as a low-cost, sustainable, and efficient material for heavy metal remediation. Further work should consider adsorbent regeneration and reuse, competitive adsorption in multi-metal systems, and large-scale testing with real wastewater.

Compliance with ethical standards

Disclosure of conflict of interest

No conflict of interest to be disclosed.

References

[1] S. Babel and T. A. Kurniawan, "Low-cost adsorbents for heavy metals uptake from contaminated water: A review," *Journal of Hazardous Materials*, vol. 97, no. 1-3, pp. 219-243, 2003.

[2] K. Y. Foo and B. H. Hameed, "Insights into the modeling of adsorption isotherm systems," *Chemical Engineering Journal*, vol. 156, no. 1, pp. 2-10, 2010.

[3] Y. S. Ho and G. McKay, "Pseudo-second order model for sorption processes," *Process Biochemistry*, vol. 34, no. 5, pp. 451-465, 1999.

[4] A. Demirbas, "Heavy metal adsorption onto agro-based waste materials: A review," *Journal of Hazardous Materials*, vol. 157, no. 2-3, pp. 220-229, 2008.

[5] V. K. Gupta and I. Ali, *Environmental Water: Advances in Treatment, Remediation and Recycling*. Amsterdam, The Netherlands: Elsevier, 2012.

[6] H. N. Tran, S.-J. You, and H.-P. Chao, "Fast and efficient adsorption of methylene green 5 on activated carbon prepared from new chemical activation method," *Journal of Environmental Management*, vol. 188, pp. 322-336, 2017.

[7] J. Wang and X. Guo, "Adsorption isotherm models: Classification, physical meaning, application and solving method," *Chemosphere*, vol. 258, Art. no. 127279, 2020.

[8] Y. Liu, Y.-J. Liu, and X. Guo, "Thermodynamic and kinetic analysis of heavy metal adsorpion by biomass-derived adsorbents," *Environental Science and Pollution Research*, vol. 28, no. 15, pp. 18467-18479, 2021.

[9] M. A. Ahmad, W. M. A. Wan Daud, and M. K. Aroua, "Adsorption of heavy metals on activated carbons prepared from agricultural waste biomass: A review," *Journal of Environmental Chemical Engineering*, vol. 1, no. 3, pp. 339-348, 2013.

[10] M. Danish and T. Ahmad, "A review on utilization of wood biomass as a sustainable precursor for activated carbon production and application," *Renewable and Sustainable Energy Reviews*, vol. 87, pp. 1-21, 2018.

[11] N. A. Rashidi and S. Yusup, "An overview of activated carbon production from biomass by chemical activation with phosphoric acid," *Journal of Analytical and Applied Pyrolysis*, vol. 134, pp. 1-16, 2018.

[12] M. Hua, S. Zhang, B. Pan, W. Zhang, L. Lv, and Q. Zhang, "Heavy metal removal from water/wastewater by nanosized metal oxides: A review," *Journal of Hazardous Materials*, vols. 211-212, pp. 317-331, 2012.

[13] M. Kobya, E. Demirbas, E. Senturk, and M. Ince, "Adsorption of heavy metal ions from aqueous solutions by activated carbon prepared from apricot stone," *Bioresource Technology*, vol. 96, no. 13, pp. 1518-1521, 2005.

[14] J. Acharya, J. N. Sahu, C. R. Mohanty, and B. C. Meikap, "Removal of lead(II) from wastewater by activated carbon developed from Tamarind wood by zinc chloride activation," *Chemical Engineering Journal*, vol. 149, no. 1-3, pp. 249-262, 2009.

[15] M. Imamoglu and O. Tekir, "Removal of copper(II) and lead(II) ions from aqueous solutions by adsorption on activated carbon from a new precursor hazelnut husks," *Desalination*, vol. 228, no. 1-3, pp. 108-113, 2008.

[16] A. Bhatnagar and M. Sillanpää, "Utilization of agro-industrial and municipal waste materials as potential adsorbents for water treatment—A review," *Chemical Engineering Journal*, vol. 157, no. 2-3, pp. 277-296, 2010.

[17] G. Crini, "Non-conventional low-cost adsorbents for dye removal: A review," *Bioresource Technology*, vol. 97, no. 9, pp. 1061-1085, 2006.

[18] D. Mohan and C. U. Pittman Jr., "Activated carbons and low cost adsorbents for remediation of tri- and hexavalent chromium from water," *Journal of Hazardous Materials*, vol. 137, no. 2, pp. 762-811, 2006.